Calculation of the dynamics of drug binding in a netropsin-DNA complex

Y. Z. Chen and E. W. Prohofsky
Department of Physics, Purdue University, West Lafayette, Indiana 47907-1396
(Received 20 January 1995)

We calculate the drug binding constant and thermal fluctuational base pair opening probabilities of a netropsin-bound DNA polymer poly $d(GATATC)$·poly $d(GATATC)$ at room temperature (293 K). For comparison we also calculate the probabilities for the free DNA helix. The calculation is carried out by a statistical approach using microscopic structure and established dynamic force fields. The analysis of netropsin binding or dissociation involves calculations of the disruption of several different elements that bind the drug to the DNA helix including hydrogen bonding, the nonbonded attraction in the minor groove, and a conformational factor. Good agreement between our calculated and the observed drug binding constant occurs for a reasonable choice of H-bond parameters for the complex in a solution. Our calculation also shows that the opening probability of the base pairs near the binding site is significantly reduced by a variety of interactions between the helix and the drug.

PACS number(s): 87.15.By, 63.20.Dj, 63.70.+h, 87.15.Kg

I. INTRODUCTION

The biological behavior of the DNA double helix is greatly affected by drugs and other protein molecules that bind to it. The complexes have altered dynamics from that of the free helix and free molecule. One area of interest is the dynamics of the binding of the complex itself and another is the change in the dynamics of the helix brought about by the binding of the molecule. In this paper we study the binding and dissociation probability of a netropsin molecule to a section of helix and the change in helix stability against base pair separation brought about by the binding. The stability against base pair opening for a similar section of the drug free helix is also shown for comparison.

Such an analysis involves calculations of the disruption of several different elements that bind the complex, such as H bonds, van der Waals interactions, and Coulomb interactions. In an earlier work, the separation of daunomycin from DNA, the analysis also involved the problem of extraction of an intercalated structure of the drug from the stacked DNA base pairs [1]. As will be shown in this paper the current problem involves the disruption of H bonds coupled to a conformation change of the drug, followed by a dissociation of the drug from the DNA minor groove. All these processes occur in large complex systems where the disruption processes are determined by the collective dynamics of the large systems. The dynamics of disruption of an H bond that is part of a large system is different from the dynamics of he disruption of a similar bond in a system of just a few atoms. Large system dynamics are determined by collective excitations of the large system.

To our knowledge there has been no satisfactory theoretical approach to the problem of bond disruption and separation of large entities containing information on the level of individual atoms for processes that occur on relatively long time scales. For example, base pair separation in DNA requires analysis of dynamics on a millisecond time scale [2]. Molecular dynamic simulation does give information on an atomic level of detail, but cannot come close to being run for milliseconds of simulated time for large systems. Simpler thermodynamic analysis does not give information on the atomic level and does not lead to further insights of dynamics on the molecular level. Also the input thermodynamic information is in terms of thermodynamic parameters that are not simple to interpret in terms of individual atom-atom interactions and motions. The method developed here can predict the complex separation of large entities based only on starting information that includes conformational structure and atom-atom interaction potentials. The method has been used in helix melting calculations [3] and the dissociation of an anticancer drug daunomycin from DNA [1].

The method presented here achieves applicability to long time scale events by determining equilibrium values for the mean atom displacements and the mean probability of bond disruption. The problems that stopped the application of statistical mechanics to problems of bond disruption in large systems were the inability to properly specify the form of interatom interaction and the difficulty in dealing with the dynamics of large systems with highly nonlinear interactions. The method applied here solves both these problems and leads to a statistical analysis that has proven to work very well in calculating the dynamics of DNA melting in a number of different situations. Although the method appears to be a dynamic calculation, it is a mixed dynamic thermodynamic one. The criterion used in setting up the calculation is that it will lead to solutions that give the best approximation to the true free energy. Entropic effects are included in the solution by incorporating statistical mechanics into the definition of the effective potentials used in the dynamic solution.

The difficulty in specifying interatom interactions arises because of the way statistical mechanics responds to bounded and unbounded interactions. Systems con-

nected by bounded interactions are always predicted to be dissociated by straightforward statistical methods, even at infinitesimal temperatures [4]. Systems connected by unbounded potentials, like quarks, are incapable of melting at any temperature. We solve this problem by using effective phonon harmonic interactions modified by a bond breaking operator [3]. The problem of dealing with large numbers of nonlinear interactions is also solved in the context of effective phonon theory in which self-consistency is used to incorporate nonlinearities into effective harmonic interactions, which can then be analyzed by harmonic methods suited to large systems [5].

Since the analysis is carried out at the atomic level of detail it is possible to calculate the probability of dissociation of each H bond and each other element in the overall dissociation. It is possible, in the netropsin-DNA case, to calculate the disruption of the H bonds that holds the drug to a specific site and separately calculate the events that are required for the drug to leave the minor groove. The combined probability can then be calculated as the drug-helix dissociation probability, which can be inverted to give the drug-helix binding constant.

Even with disrupted H bonds the netropsin is bound nonspecifically to the minor groove by two factors, the nonbonded attraction to the groove and a conformal factor. As shown in Fig. 1 the bound conformation essentially is something of a C clamp in that it surrounds the helix in a way that does not allow separation without conformational distortion of the netropsin. We calculate the probability of a model conformation change that allows drug-helix separation and the probability of dissociation from the minor groove with the C-clamp effect relaxed. It is the probability of these two events times that of the probability of specific H-bond disruption that leads to the total dissociation probability.

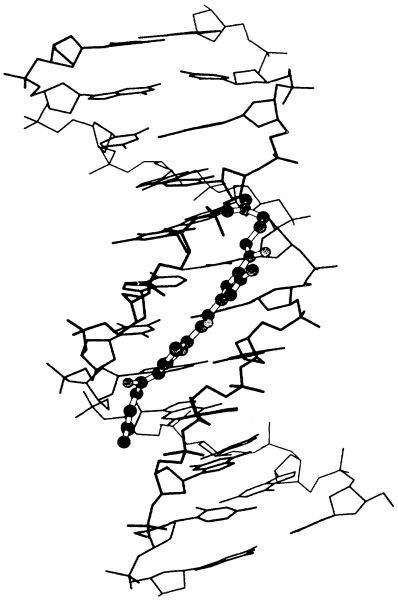

FIG. 1. X-ray crystal structure of a netropsin-*d*(*CGCGATATCGCG*) complex. The netropsin drug (ball and stick) is seen to bind tightly and forms a C-clamp in the minor groove of DNA (line drawing). The C18 end of the drug (upper end in the figure) is bent and extends to the other side of the helix. This makes it impossible for the drug to be displaced from the DNA minor groove without a conformation change to avoid the clash between the drug and DNA phosphate group. This graphic was generated by MOLSCRIPT [30] [Kraulis, J. Appl. Crystallogr. **24**, 946 (1991)].

Netropsin and its interaction with DNA have received extensive study in recent years [6–12]. Netropsin exerts its biological activity by binding tightly to the minor groove of *B*-DNA double helices, hence interfering with both replication and transcription. Netropsin binding involves structural and electrostatic components, in addition to drug-base hydrogen bonding and van der Waals interactions. As shown in the present work, these components play important roles in the dynamic stability of netropsin binding, which can be formulated in the framework of the effective harmonic theory.

The dissociation of netropsin from the minor groove is hindered by the presence of sugar-phosphate groups located at the outer edge of the minor groove, i.e., the conformational factor. As shown in Fig. 1, in order to overcome this barrier a substantial change in the dihedral angles at one end of the drug is necessary before the final separation of the drug. Such a change enables the end of the drug to swing out of the minor groove to avoid the hindrance from the sugar-phosphate groups in advance of the final translational separation. It also allows the drug to relax to its free conformation, as shown in Fig. 2. Crystallographic analysis indicates that substantial dihedral angle changes occur widely in proteins [13]. Therefore a study of the thermal fluctuational motions in netropsin not only is important for the determination of netropsin dissociation but can also shed light on the role of such motions in protein folding and unfolding processes.

In the crystal structure used to construct our netropsin-DNA complex, one end section of netropsin seems to be compressed into the minor groove because of crystal packing. The distances in the drug-base H bond in the section are much shorter than that found for H

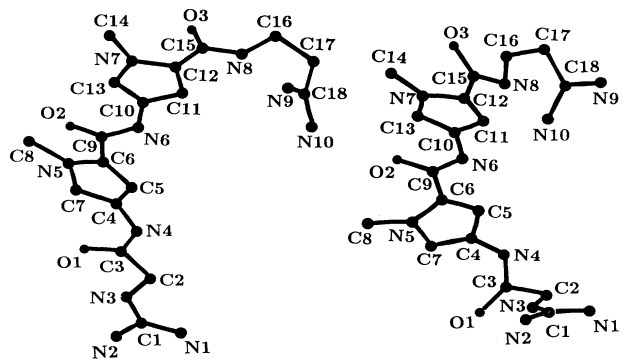

FREE NETROPSIN DNA-BOUND NETROPSIN

FIG. 2. Comparison between the structure of a free netropsin and that of a netropsin bound to DNA.

bonding. We assume that in solutions where dissociation is possible, this strong crystal field effect is relaxed and that the H-bond potentials found for other systems can be used. Our potential would indicate a solution H-bond length of 2.78 Å compared to the crystal structure length of 2.70 Å.

Several experiments [14,15] seem to indicate that electrostatic interactions between the two cationic ends of netropsin and DNA contribute to the stability of the binding drug. It was found that netropsin modifications with the cationic ends removed, and analogs with cationic ends but without drug-base H-bonding capabilities, show both an appreciable binding to *B*-DNA and base specificity for *AT* base pairs. This indicates that electrostatic interactions coupled with van der Waals interactions are strong enough to sustain netropsin binding without drug-base hydrogen bonding. We will show in the present work that electrostatic interactions indeed play a substantial role in the dynamic stability of netropsin binding.

II. STRUCTURE AND FORCE FIELDS

The DNA polymer poly $d(GATATC)$·poly $d(GATATC)$ considered in this work is a linear infinite helix. The structure for the drug free helix is generated from fiber *B*-DNA data [16]. The structure for the netropsin-bound helix is from the x-ray crystal coordinates of a netropsin-$d(CGCGATATCGCG)$ complex deposited in the Brookhaven protein data bank [11]. In the netropsin-bound helix one netropsin binds to the minor groove of every *GATATC* segment. The drug-base pair (BP) ratio in our model is therefore 6 BP per drug. As these helices are composed of repeating sequence *GATATC* plus the drug, one can exploit helical symmetry to reduce the calculation to a number of calculations with the dimensionality of a unit cell that contains a six base pair *GATATC* sequence plus the drug.

In our calculation we do not explicitly consider hydrogen atoms. However, the masses and the partial charges of all the hydrogen atoms in the system are added to those of their respective parent atoms. The number of atoms per unit cell, excluding hydrogen atoms, is 246 for the free helix and 277 for the drug-bound helix. The number of atoms in netropsin is 31. The dimensionality of the reduced equation of motion is therefore 738×738 for the free helix and 831×831 for the drug-bound helix. The nomenclature for the bases in a unit cell in one strand are $G1$, $A2$, $T3$, $A4$, $T5$, and $C6$, and the complimentary bases in the opposite strand are $C12$, $T11$, $A10$, $T9$, $A8$, and $G7$. The netropsin drug is denoted as Nt.

In our calculation the valence force constants are regarded as temperature independent and are refined from a spectra study on DNA bases [17] and DNA sugar-phosphate [18]. The valence force constants for the netropsin drug are from the AMBER force fields [9,19]. The DNA interbase and drug-base H-bond force constants are determined self-consistently by an integration over the second derivative of a H-bond potential weighted by a vibrational distribution function [5]. These H-bond force constants are further scaled by $1-P_{li}$ to take into consideration the effects of disrupted bonds in a mean field theory [3]. Here P_{li} is the bond disruption probability of the ith bond in the lth base pair or drug-base connection.

The potential used to model hydrogen bonds is a Morse potential between the bond end atoms. The parameters of the Morse potential for the DNA base pairs are those used in our cooperative modified self-consistent phonon approximation (MSPA) calculations [20]. The Morse parameters for the drug-base H bonds are derived from the x-ray determined bond lengths and by the use of force constants and dissociation energies calculated from the Lippincott-Schroeder model [21]. The Morse parameters and maximum intact stretch lengths of the drug-base H bonds for the netropsin-bound helix are given in Table I.

In addition to the valance force constants and H-bond force constants, we also incorporate nearest-neighbor van der Waals and long range Coulomb interactions into our dynamic force field [22,23]. The same formula is used to construct the van der Waals and Coulomb force constants for interactions between netropsin and DNA. In deriving the Coulomb force constants involving drug atoms, we use the AMBER charges [9] for the netropsin atoms. The cooperative effect of nearest neighbors can be introduced into our base stacking force constants by scaling these force constants by a factor of $1-\sqrt{P_l^{\rm op}P_{l'}^{\rm op}}$ [3]. Here $P_l^{\rm op}$ and $P_{l'}^{\rm op}$ are base pair opening probabilities or drug dissociation probabilities of the two neighboring pairs.

III. COMPUTATION PROCEDURE AND PREMELTING BASE PAIR OPENING PROBABILITY

A detailed description of the cooperative MSPA theory used in our computation can be found in our earlier publication [3]. Here we briefly summarize the basic pro-

TABLE I. Morse parameters (a, r^0, and V^0) and maximum stretch length $L^{\max}$ of the drug-DNA H bonds in netropsin-bound poly $d(GATATC)$·poly $d(GATATC)$. The Morse potential is given as $V=V^0\{1-\exp[-a(r-r^0)]\}^2-V^0$ in which r is the distance between the two bond-end atoms.

System	Bond	a (Å^{-1})	r^0 (Å)	V^0 (kcal/mol)	$L^{\max}$ (Å)
Nt-$T3$	N4—H—O2	2.420	2.693	2.057	3.191
Nt-$A10$	N6—H—N3	2.557	2.724	2.093	3.191
Nt-$T5$	N10—H—O2	3.013	2.679	4.206	3.068
Nt-$C6$	N10—H—O2	3.091	2.670	4.273	3.068

cedure for the self-consistent calculation of vibration equation of motion and bond disruption probabilities for both free molecules and a drug-bound helix. The calculation is carried out in iteration loops involving several steps given below:

Step 1. Given the coordinates and initial force constants, one can solve the equation of motion of a molecule with helical symmetry,

$$\left[\sum_k B^{\dagger}(\theta)\Phi(\theta)B(\theta)-[\omega_\lambda(\theta)^2]I\right]q^\lambda(\theta)=0 , \quad (1)$$

where k is the index for the type of harmonic motions (valence bond stretch, angle bending, torsion, out of plane bending, H-bond breathing, and motions induced by nonbonded van der Waals and Coulomb interactions). λ is the normal mode band number. θ is introduced in the equation as a result of the reduction of the dimensionality of the system through helical symmetry. It is the phase difference between the motion of adjacent unit cells. θ runs through all values in the range $-\pi<\theta\leq\pi$, and it is related to the wavelength by wavelength$=2\pi h/\theta$. $B(\theta)$ is the transformation matrix (B matrix) from all the unit cells in mass weighted Cartesian coordinates (MWC) to the zeroth unit cell in internal coordinates, and its expression can be found in the literature [24]. $\Phi(\theta)$ is the matrix of valence force fields, H-bond force constants, van der Waals force constants, and Coulomb force constants. $\omega_\lambda(\theta)$ and $q^\lambda(\theta)$ are the eigenfrequency and eigenvector in mass weighted Cartesian coordinates, respectively.

Step 2. Using the eigenfrequencies and eigenvectors one can determine the mean-square vibrational amplitude of a bond,

$$D_{li}=\sum_\lambda \int_0^\pi d\theta \frac{|s_{li\lambda}(\theta)|^2}{2\pi\omega_\lambda(\theta)}\coth\left[\frac{\hbar\omega_\lambda(\theta)}{2K_BT}\right] , \quad (2)$$

where k_B is the Boltzmann constant, $\hbar$ is the Planck constant divided by 2π, and $s_{li\lambda}(\theta)$ is the internal stretch coordinate or the projection of the difference of end-atom eigenvectors onto bond orientation [24]. l is the index for the base pair or drug-base connection in a unit cell, and i is the index of the bonds in the system.

Step 3. After determination of D_{li} one can determine the equilibrium bond length R_{li},

$$R_{li}=(1-P_l^{\rm uc})\{r_{li}^0+\frac{1}{a_{li}}\ln[\cosh(\mu_{li}a_{li})]\} +P_l^{\rm uc}(L_{li}^{\max}+2P_{li}\sqrt{2D_{li}}) \quad (3)$$

and bond disruption probability P_{li},

$$P_{li}=C_{li}\int_{L_{li}^{\max}}^\infty dr\exp\{-(r-R_{li})^2/2D_{li}\} . \quad (4)$$

In Eq. (3) $\mu_{li}=2\sqrt{2D_{li}\ln 2}$ and r_{li}^0 and a_{li} are the parameters of the Morse potential we have chosen to model the H-bond interaction. $P_l^{\rm uc}$ is the base pair unconstrained probability [3], which is given as $P_l^{\rm uc}=(P_{l-1}^{\rm op}P_l^{\rm op}P_{l+1}^{\rm op})^{1/3}$, and $P_l^{\rm op}$ is the base pair opening probability given below. In Eq. (4) C_{li} is a normalization factor given in our earlier publication and $L_{li}^{\max}$ is the maximum bond stretch length before disruption.

Step 4. Using the calculated D_{li} and R_{li} one can calculate a new intact bond force constant as

$$\phi_{li}^{\rm int}=C_{li}\int_{r_{li}^{\min}}^\infty dr\exp\{-(r-R_{li})^2/2D_{li}\}\frac{d^2V(r)}{dr^2} , \quad (5)$$

where $r_{li}^{\min}$ is the hard-core inner boundary and $V(r)$ is the potential for the bond end atoms.

Step 5. Using the calculated P_{li}'s one can determine premelting thermal fluctuational base pair opening probability or drug dissociation probability $P_l^{\rm op}$. For a drug-free base pair its $P_l^{\rm op}$ is given by the product of the P_{li}'s of its interbase H bonds,

$$P_l^{\rm op}=\prod_i P_{li} . \quad (6)$$

In the netropsin-bound poly $d(GATATC)$·poly $d(GATATC)$ there are several H bonds bridging between the drug and the bases [11]. Between the $T3$-$A10$ base pair and netropsin there are two such bonds. One is the O2($T3$)—H—N4(Nt) bond and the other is the N3($A10$—H—N6(Nt) bond. These drug-base H bonds restrict the motion of the $T3$ and $A10$ bases. As a result the opening of the $T3$-$A10$ base pair requires the simultaneous disruption of its interbase H bond and the two drug-base H bonds. The opening probability is then

$$P_{C2\text{-}G7}^{\rm op}=P_{\rm O2(T3)—H—N4(Nt)}P_{\rm N3(A10)—H—N6(Nt)} \times\prod_i P_{T3\text{-}A10,i} . \quad (7)$$

A H bond forms between the O2 atom of the $T5$ base and the N10 atom of netropsin. The opening probability of the $T5$-$A8$ base pair is then

$$P_{T5\text{-}A8}^{\rm op}=P_{\rm O2(T5)—H—N10(Nt)}\prod_i P_{T5\text{-}A8,i} . \quad (8)$$

Another H bond is found between the O2 atom of the $C6$ base and the N10 atom of netropsin. The opening probability of the $C6$-$G7$ base pair is therefore

$$P_{C6\text{-}G7}^{\rm op}=P_{\rm O2(C6)—H—N10(Nt)}\prod_i P_{T5\text{-}A8,i} . \quad (9)$$

Using the calculated probabilities one can scale the force constants as described in the preceding section. The scaled force constants are then used to repeat the calculation from steps 1–5. This iteration process continues until a self-consistent solution is found for the force constants. In our calculations a self-consistency is assumed if the difference between the force constants of the current iteration and previous iteration divided by the force constant is less than 0.003 at premelting temperatures and less than 0.006 near the melting temperature.

IV. FORMULATION OF NETROPSIN DISSOCIATION

A. Dissociation pathway and determination of potential

The attachment of netropsin to the minor groove has several distinct elements, H bonds, van der Waals interactions and Coulomb interactions. The H-bond interactions are unique in that they are of a much shorter

range than the others and are found to be disrupted by fluctuational displacements of tenths of angstroms, as can be seen in Fig. 3. The other interactions require much larger displacements for disruption, and this scaling difference imposes a hierarchy of events on the total disruption. The H bonds will be disrupted before the fluctuations leading to disruption of the other factors becomes possible. The calculation of the H-bond dissociation then is carried out with all other interactions present, but the further separation is calculated with the assumption that the H bonds are disrupted. The overall disruption probability is then the product of the independent probability that the H bonds are disrupted times the conditional probability of all other elements being disrupted; the conditional probability is that of the other elements disrupting, given that the H bonds are disrupted. This conditional probability is calculated as the separation of the netropsin in a composite potential of van der Waals and Coulomb interactions but without H bonds.

This last separation also involves two separable elements. As shown in Fig. 2 the bound netropsin is in a distorted conformation compared to that found for free netropsin [11,25]. From Fig. 1 we find that the bound conformation cannot simply be displaced from the DNA minor groove without generating a clash between atoms of netropsin and those of the Helix phosphate group. A conformation change in the direction of the free netropsin conformation will allow for separation of the drug from the helix. The required differences in conformation can be brought about in the simplest and least energy costly manner by a rotation of two dihedral angles at the C18 end of the drug near the *T*5-*A*8 pair of the DNA. One of the angles is that between the plane determined by the C18—C17 and C17—C16 bonds and that plane determined by the C17—C16 and C16—N8 bonds. The other dihedral is between the plane determined by the C17—C16 and C16—N8 and the plane of the C16—N8 and N8—C15 bonds. A rotation of 90° and 60° of each of these dihedral angles will bring about the required conformation change. The dissociation of netropsin would then first require disruption of the drug-DNA H bonds, followed by a conformation change in the netropsin, followed by translation of the altered drug from the DNA minor groove. The total dissociation probability is then given by the product of these separate events. To simplify the calculation of the last step, the translation of the drug out of the minor groove is carried out using an approximation of a composite potential rather than a full many body solution of all the individual atoms in the problem. This same approximation seemed to work well in a similar calculation on the dissociation of daunomycin from DNA. [1].

This composite potential well can be constructed by combining all the atom-atom van der Waals and Coulomb potentials as a function of a displacement of the drug along a specific path. For the van der Waals potential we use a Lennard-Jones 6-12 potential. The parameters of this potential for the atoms of both DNA and netropsin are from AMBER data [9,19]. For the Coulomb potential the charges for the atoms in DNA are from Miller [26] and the charges for the atoms in netropsin are from AMBER data [9]. The determination of the dielectric constants is a nontrivial problem. In simulation studies of DNA's and proteins [19] dielectric constants are taken as distance dependent: $\varepsilon = r_{ij}$. However, a DNA binding netropsin is in the interface between the floor of the minor groove and the bulk water. Therefore a dielectric constant appropriate for protein and nuclei acids is insufficient in describing the effect of the partial shielding by bulk water. In our earlier study of the salt dependent melting of DNA [27] we find that Coulomb interactions involving atoms at the interface between DNA and bulk water are best described by a dielectric constant, which is a geometric mean of the bulk water dielectric constant and that of DNA. In the present study we employ the same formalism to use a dielectric constant $\varepsilon = \sqrt{r_{ij}\varepsilon_{\text{water}}}$ in our drug-DNA Coulomb interaction. The distance dependent dielectric constant is incorporated in our model of composite Coulomb potential because the charges used in our study are from simulations that use distance dependent dielectric constants.

B. Dissociation probability

Based on the discussion in Sec. IV A the netropsin dissociation probability P_D can given by

$$P_D = P_{\text{Nt—H-bs}} P_{\text{Nt-rot}} P_{\text{Nt-trans}} , \tag{10}$$

where $P_{\text{Nt—H-bs}}$ is the probability of the simultaneous disruption of all the drug-base H bonds and it is given by the product of the probabilities of individual drug-base H bonds,

$$P_{\text{Nt—H-bs}} = P_{\text{N4—H—O2}(T3)} P_{\text{N6—H—N3}(A10)} \times P_{\text{N10—H—O2}(T5)} P_{\text{N10—H—O2(C6)}} . \tag{11}$$

The individual drug-base H-bond disruption probabilities are determined by the same formula as for the DNA interbase H bonds given in the preceding section.

$P_{\text{Nt-rot}}$ is the probability of a sufficient rotational conformation change occurring in the C18 end of netropsin after the disruption of drug-base H bonds, and it is given as

$$P_{\text{Nt-rot}} = P_{\text{dihedral C18,C17,C16,N8}} P_{\text{dihedral C17,C16, N8,C15}} , \tag{12}$$

in which P_{dihedral} is the probability of the dihedral angle to displace beyond a critical angle, and is given by

$$P_{\text{dihedral}} = C_\phi \int_{\phi_{\max}}^{\phi_{\text{out}}} d\tau \exp[-(\tau-\phi)^2/2D_\phi] . \tag{13}$$

In the above equation $\phi_{\max}$ is the critical angle beyond which the end section is considered to rotate out of the minor groove, and its value will be given below. ϕ_{out} is the outerbound of the dihedral angle. C_ϕ is the normalization factor given by $C_\phi^{-1} = \int_{\phi_{\text{in}}} d\tau \exp[-(\tau-\phi)^2/2D_\phi]$ in which ϕ_{in} is the inner bound of the dihedral angle. D_ϕ is the mean square vibrational dihedral angle displacement given by

$$D_\phi \equiv \langle (\Delta\phi)^2 \rangle = \sum_\lambda \int_0^\pi d\theta \frac{|s_\phi^\lambda(\theta)|^2}{2\pi\omega_\lambda(\theta)} \coth\left[\frac{\hbar\omega_\lambda(\theta)}{2K_B T}\right], \tag{14}$$

where $\hbar$ is the Planck constant divided by 2π. $s_\phi^\lambda(\theta)$ is the internal coordinate for the dihedral displacement, and is taken from MSPA self-consistently calculated eigenvectors. The relationship between $s_\tau^\lambda(\theta)$ and the eigenvectors in MWC coordinates can be found in the literature [24]. The dihedral angle ϕ can be given as

$$\phi = \phi_0 + \Delta\phi , \tag{15}$$

where ϕ_0 is the x-ray determined dihedral angle and $\Delta\phi$ represents the dihedral angle displacement. $\Delta\phi$ is determined such that $V_\phi(\phi_0+\Delta\phi+\mu) = V_\phi(\phi_0+\Delta\phi-\mu)$. V_ϕ is the potential for the dihedral motion,

$$\begin{aligned} V_\phi &= \frac{V_n}{2}[1+\cos(n\phi-\gamma)] + V_{nb}(\phi) \\ &= \frac{V_n}{2}[1-\cos[n(\phi-\phi_0)+\delta]] + V_{nb}(\phi) , \end{aligned} \tag{16}$$

where V_n, n, and γ are the parameters from AMBER [9,19] and are given in Table II. $\delta = n\phi_0 - \gamma - 180°$ and $V_{nb}(\phi)$ are the nonbonded van der Waals and Coulomb potentials, between the drug-end atoms and the DNA. The potential V_ϕ for the two dihedral angle rotations in the drug end is shown in Figs. 3 and 4, respectively. As in our earlier studies we define μ as the full width at half maximum of the distribution function $\exp(-u^2/D_\phi)$, which gives $\mu = 2\sqrt{2D_\phi \ln 2}$. Finally $\phi_{\max}$ is taken as the first inflection point of the potential without the H bonds (the chain-dot line in Fig. 3 and the solid line in Fig. 4), and its value is given in Table II. Here inflection point refers to the point where the second derivative of the potential becomes zero. We find from Fig. 3 that the combined potential of the two drug-base N10—O2 H bonds is deep and narrow compared to the other potentials. Therefore the disruption of these two H bonds is necessary before larger values of the dihedral angle can be sampled, leading to the disruption of other interactions.

TABLE II. Parameters (V_n, n, γ, and δ) for the dihedral potential, x-ray dihedral angle ϕ_0, and the critical dihedral angle $\phi_{\max}$ at the C18 end of netropsin bound to poly $d(GATATC)$·poly $d(GATATC)$.

Parameter	C18—C17—C16—N8	C17—C16—N8—C15
V_n (kcal/mol)	4.0	0.0
n	3	3
γ (degree)	0.0	0.0
δ (degree)	14.0	−76.0
ϕ_0 (degree)	64.6	154.6
$\phi_{\max}$ (degree)	89.9	110.0

The relative weights of the two contributions of van der Waals and Coulomb potentials are shown in Figs. 3 and 4 for a range of dihedral angles. The Coulomb interaction is far larger than the van der Waals interaction and is roughly three-quarters of the combined potential. Clearly Coulomb interactions are significant in the conformational locking of the drug to the helix.

$P_{\text{Nt-trans}}$ is the probability for the drug final translational separation from the minor groove. It can be determined by assuming that, after the disruption of all the drug-base H bonds and the rotation of the C18 end of the drug, the bulk drug can oscillate in and out of the minor groove in the calculated composite potential well. The orientation of the drug final translational movement is chosen as along the line between the C8 atom and the C6 atom of the drug. This orientation is approximately pointing directly out of the minor groove at the middle

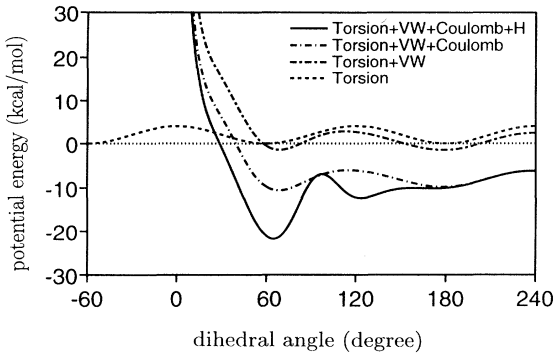

FIG. 3. Potential energies for the dihedral movement in C18—C17—C16—N8 bond of the netropsin bound to poly $d(GATATC)$·poly $d(GATATC)$. The x-ray observed dihedral angle is 60.4°. The solid line corresponds to the total potential including torsion, van der Waals, Coulomb, and H-bond energies. The chain-dot line corresponds to the potential of torsion, van der Waals, and Coulomb. The chain-dashed line corresponds to the torsion plus van der Waals potential. The dashed line correspond to the torsion potential. The second minima at $\approx 120°$ in the solid line is due to the N10—H—O2(C12) H bond. The N10—H—O2(C12) bond has two minima in the range of dihedral angle rotation.

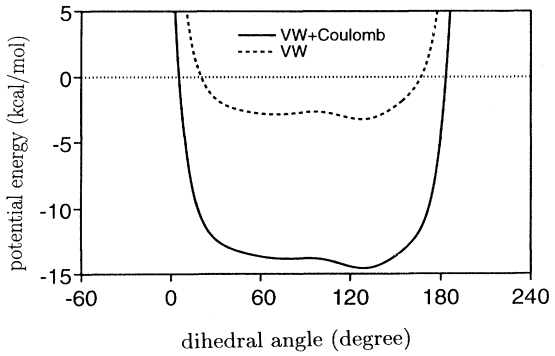

FIG. 4. Potential energies for the dihedral movement in the C17-C16-N8-C15 bond. These potentials are calculated by assuming the dihedral angle of the C18-C17-C16-N8 bond is displaced 90° out of the minor groove. The torsion potential given in the AMBER force field is zero at all angles and is not shown in the figure. The x-ray observed dihedral angle is 154.6°. The solid line correspond to the van der Waals and Coulomb potential. The dashed line corresponds to the van der Waals potential.

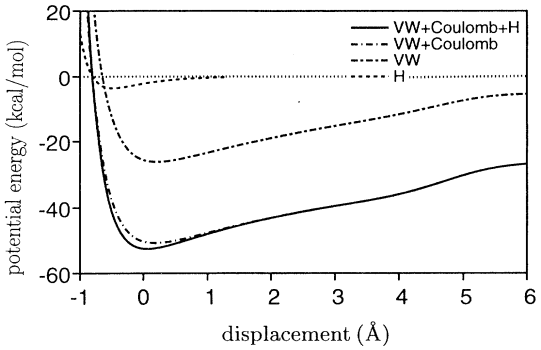

FIG. 5. Potential energies for the final translational displacement of a DNA-bound netropsin after the rotation of its C18 end out of the minor groove. The displacement is the center of mass displacement of the drug along the orientation between the C8 and C6 atom o the drug with respect to the x-ray observed position. The positive displacement corresponds to the dissociation of the drug from the minor groove and the negative the movement of the drug further into the minor groove. The H-bond energy is for the N4-H-O2 and N6-H-N3 bonds only, as the other two drug-base H bonds are disrupted after the rotation of the drug C18 end. The solid line corresponds to the total potential energy including van der Walls, Coulomb, and H-bond energy. The chain-dot line corresponds to the van der Waals and Coulomb potential. The chain-dash line corresponds to the van der Waals potential and the dashed line the H-bond potential.

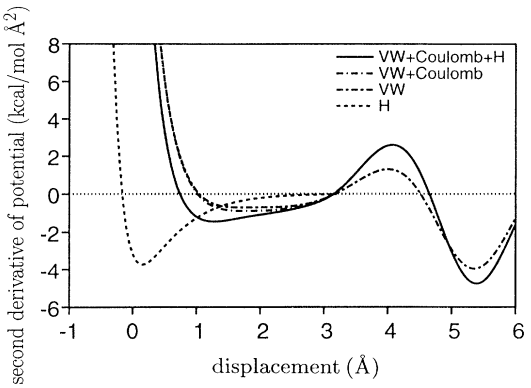

FIG. 6. Second derivatives of the potential energies described in Fig. 3. The lines refer to the same potential energies given in Fig. 3.

section of the drug. Figure 5 displays several composite potentials of the drug (with the C18 end rotated out of the minor groove) as a function of the center of mass displacement from its x-ray position along the specified orientation. The potentials in the figure include the van der Walls potential, the Coulomb potential, and the combination of both, together with the combined potential with drug-base H bonds included. The second derivatives of these potentials are given in Fig. 6. In these figures the positive displacement corresponds to the movement of the drug out of the minor groove, and the negative displacement corresponds to the movement of the drug further into the minor groove. We find from Figs. 5 and 6 that drug-base H bonds are only of significance for very small drug displacement. This indicates that van der Waals and Coulomb interactions play the important role in the dynamical stability against final separation.

The final translational motion of the drug in and out of the minor groove can be described in a similar way as that used to model the unstacking of an intercalating drug daunomycin [1]. As discussed in Sec. IV A this translational motion can be assumed to be directed approximately along the C8-C6 orientation. This motion can be described by an effective one dimensional MSPA harmonic Hamiltonian,

$$H_0=\tfrac{1}{2}M\dot{u}^2+\tfrac{1}{2}\phi_{\text{trans}}u^2 , \tag{17}$$

where M is the total mass of the drug and u is the center of mass displacement around an equilibrium center of mass position R. $R=R_0+\Delta R$, where R_0 is the x-ray observed position and ΔR is the mean displacement of the drug after the disruption of the drug-base H bonds and the rotation of the lower drug end. It is determined self-consistently, as shown below. In accordance with Figs. 5 and 6 we set R_0 equal to zero. ϕ_{trans} is the effective force constant determined by minimizing the variational free energy $F=F_0+\langle H-H_0\rangle$. F_0 is the free energy of the effective harmonic system Eq. (17): $F_0=-k_BT\ln[\exp(-H_0/k_BT)]$. T is the temperature and k_B is Boltzmann's constant.

The stationary condition $\partial F/\partial D=0$ ($D=\langle u^2\rangle$) then gives

$$\phi_{\text{trans}}=(1-P_{\text{Nt-trans}})\times\frac{\int_{L_{\min}}^{\infty}due^{-u^2/2D}\frac{d^2}{du^2}V(\Delta R+u)}{\int_{L_{\min}}^{\infty}due^{-u^2/2D}} , \tag{18}$$

where V is the composite van der Waals and Coulomb potential described in Fig. 5 (chain-dot line), and $L_{\min}$ is the inner bound of the hard core of the potential chosen as -1 Å. $1-P_{\text{Nt-trans}}$ is used to scale the force constant to take into consideration the effect of dissociated drugs in our mean field theory. The mean-square vibrational displacement D can be given from another stationary condition, $\partial F/\partial\phi_{\text{trans}}=0$, which gives

$$D=\frac{qq^*}{2M\omega}\coth\left[\frac{\hbar\omega}{2k_BT}\right] , \tag{19}$$

where $\hbar$ is Planck's constant divided by 2π, ω is the frequency obtained from $M\omega^2=\phi_{\text{trans}}$, q is the normalized eigenvector of the Hamiltonian H_0, and $qq^*=1$ for a one dimensional system.

The mean displacement ΔR of the drug is determined by the classical condition that at the classical turnaround point, all the energy of the oscillator is stored in potential energy: $V_D(\Delta R+\mu)=V_D(\Delta R-\mu)$. As in our earlier studies we define μ as the full width at half maximum of the distribution function $\exp(-u^2/2D)$, which gives $\mu=2\sqrt{2D\ln 2}$. Finally the $P_{\text{Nt-trans}}$ can be determined by the distribution function $\exp(-u^{-2}/2D)$ as

TABLE III. Calculated netropsin equilibrium binding constant K_{eq}, dissociation probability P_D, and other probabilities of netropsin-bound poly $d(GATATC)$·poly $d(GATATC)$ at 293 K. K_{eq} is derived from $K_{eq}=(1-P_D)/P_D$, and the definition for the other probabilities can be found in the text. The experimentally estimated K_{eq} is 2.84×10^8 (Ref. [10]).

Binding constant	K_{eq}	1.81×10^8
Dissociation probability	P_D	5.52×10^{-9}
Total drug-base H-bond disruption probability	$P_{Nt—H\text{-}bs}$	6.36×10^{-6}
C18-end rotational separation probability	$P_{Nt\text{-}rot}$	2.84×10^{-1}
Final translational separation probability	$P_{Nt\text{-}trans}$	2.93×10^{-3}

$$P_{Nt\text{-}trans}=C\int_{L_{max}}^{\infty} du\ \exp[-(u-\Delta R)^2/2D]\ , \qquad (20)$$

where C is a normalization factor given by $C^{-1}=\int_{L_{min}}^{\infty} du\ \exp[-(u-\Delta R)^2/2D]$. L_{max} is the maximum displacement before dissociation. It is chosen as the first inflection point of the potential, i.e., the point where the second derivative is zero. From Fig. 6 (the chain-dot line) we find L_{max} to be 1.05 Å. L_{min} is the inner bound of the hard core in the minor groove and is chosen as -1 Å. The $P_{Nt\text{-}trans}$ is calculated by solving Eqs. (17)–(20) until self-consistency is reached.

V. RESULTS AND DISCUSSIONS

A. Netropsin binding constant

Using the formulation outlined in Sec. IV we calculate the various drug dissociation probabilities in our netropsin-DNA complex. In particular, the calculated drug dissociation probability P_D can be used to determine the equilibrium drug binding constant K_{eq}.

$$K_{eq}=\frac{1-P_D}{P_D}\ . \qquad (21)$$

The calculated probabilities and K_{eq} are shown in Table III. From Table III we find that our calculated K_{eq} is 1.81×10^8 at 293 K, which is in fair agreement with the observed value of 2.84×10^8 for the netropsin-$d(CGCAATTCGC)_2$ decamer at 298 K [10].

In the calculation of the drug final separation probability $P_{Nt\text{-}trans}$ we included Coulomb interactions in the composite potential. To examine how important Coulomb interactions are in the dynamical stability of the binding netropsin, we carried out a calculation in which only the van der Waals interactions are included in the composite potential. We find that without electrostatic interactions the calculated $P_{Nt\text{-}trans}$ is 0.0239, which is compared to the value of 0.002 93 with Coulomb interactions included. Electrostatic interactions are calculated to decrease the $P_{Nt\text{-}trans}$ and thus P_D by an order of magnitude. Consequently it increases the K_{eq} by an order of magnitude. This increase is particularly significant in the dynamic stability of a netropsin modification without drug-base H bonds. If all the drug-base H bonds are taken away we find that the K_{eq} would be 3.95×10^2 without Coulomb interactions. It becomes 3.22×10^3 when Coulomb interactions are included.

B. Effect of netropsin binding on base pair opening probability

The calculated P^{op} for the base pairs of both drug-free and netropsin-bound DNA polymer poly $d(GATATC)$·poly $d(GATATC)$ is given in Table IV. The calculated disruption probability for individual H bonds together with the equilibrium bond length and the bond vibrational mean-square amplitude for the two helices are given in Table V. The P^{op}s for the AT pairs with no hydrogen bonding to the drug are in the order of 10^{-3}, as there is no spine of hydration in the minor groove of these AT pairs [28]. We find from Table IV that base pair opening probabilities are very sensitive to netropsin binding. Netropsin binding significantly enhances the thermal stability of the base pairs at the binding site. This enhancement occurs both because of direct drug-base hydrogen bonding and because of nonbonded attractions between the drug and DNA. The calculated enhancement of the base pair thermal stability is in agreement with the observation that netropsin binding significantly increases the melting temperature of DNA [10].

X-ray analysis of a netropsin-$d(CGCGATATCGCG)$ crystal [11] indicates that there are four nonbifurcated hydrogen bonds between netropsin and the bases. Two such bonds are found to be strong and form a bridge between the drug and the $T5$-$A8$ base pair. The other two are very weak characterized by long bond lengths, and they connect the drug to the $T3$-$A10$ base pair. Our cal-

TABLE IV. Opening probability P^{op} of the base pairs in netropsin-bound and drug-free poly $d(GATATC)$·poly $d(GATATC)$ at 293 K. For comparison the P^{op} for the base pairs of a drug-free but deformed (having the same conformation as a netropsin-bound helix) poly $d(GATATC)$·poly $d(GATATC)$ are also included.

	P^{op}		
Base pair	Drug-bound	Drug-free	Free-deformed
$G1$-$C12$	7.26×10^{-6}	4.80×10^{-6}	1.00×10^{-5}
$A2$-$T11$	1.94×10^{-3}	3.19×10^{-3}	2.70×10^{-3}
$T3$-$A10$	2.42×10^{-4}	3.69×10^{-3}	3.69×10^{-3}
$A4$-$T9$	2.63×10^{-3}	3.70×10^{-3}	3.95×10^{-3}
$T5$-$A8$	1.59×10^{-6}	3.19×10^{-3}	3.63×10^{-3}
$C6$-$G7$	8.43×10^{-6}	4.81×10^{-6}	1.00×10^{-5}

TABLE V. Disruption probability P_{li}, equilibrium bond length R_{li}, and vibrational mean-square amplitude D_{li} of the interbase H bond and drug-base H bond in netropsin-bound and drug-free poly $d(GATATC)$·poly $d(GATATC)$ at 293 K.

		Drug-bound			Drug-free		
System	Bond	P_{li}	R_{li} (Å)	D_{li} (Å^2)	P_{li}	R_i (Å)	D_{li} (Å^2)
*G*1-*C*12	O6—H—N4	0.0063	2.8114	0.0165	0.0050	2.8075	0.0159
	N1—H—N3	0.0574	2.8809	0.0124	0.0375	2.8715	0.0108
	N2—H—O2	0.0223	2.8167	0.0157	0.0257	2.8201	0.0163
*A*2-*T*11	N6—H—O4	0.0333	2.8802	0.0287	0.0389	2.8857	0.0299
	N1—H—N3	0.0581	2.8923	0.0208	0.0818	2.9050	0.0236
*T*3-*A*10	O4—H—N6	0.0364	2.8832	0.0293	0.0420	2.8893	0.0305
	N3—H—N1	0.0615	2.8941	0.0212	0.0878	2.9085	0.0241
*A*4-*T*9	N6—H—O4	0.0394	2.8863	0.0300	0.0421	2.8893	0.0305
	N1—H—N3	0.0667	2.8972	0.0218	0.0878	2.9085	0.0241
*T*5-*A*8	O4—H—N6	0.0365	2.8834	0.0294	0.0390	2.8859	0.0299
	N3—H—N1	0.0716	2.8998	0.0224	0.0819	2.9052	0.0236
*C*6-*G*7	N4—H—O6	0.0063	2.8114	0.0165	0.0050	2.8075	0.0159
	N3—H—N1	0.0576	2.8810	0.0124	0.0375	2.8716	0.0108
	O2—H—N2	0.0250	2.8195	0.0162	0.0257	2.8202	0.0163
Nt-*T*3	N4—H—O2	0.2961	3.0566	0.0615			
Nt-*A*10	N6—H—N3	0.3670	3.0922	0.0808			
Nt-*T*5	N10—H—O2	0.0070	2.7818	0.0136			
Nt-*C*6	N10—H—O2	0.0087	2.7813	0.0145			

culation shows that the presence of the two strong H bonds significantly enhances the thermal stability of the *T*5-*A*8 base pair. The P^{op} of the base pair is decreased by three orders of magnitude from 3.19×10^{-3} for the drug-free helix to 1.59×10^{-6} for the drug-bound helix. The presence of the two weak H bonds also enhances the thermal stability of the binding *T*3-*A*10 but to a much lesser extent. The P^{op} of the *T*3-*A*10 base pair is decreased by only one order of magnitude from 3.69×10^{-3} for the drug-base helix to 2.98×10^{-4} for the drug-bound helix.

Although there are no hydrogen bonds between the netropsin and the *A*2-*T*11 base pair or the *A*4-*T*9 base pairs, the P^{op}*s* for these two base pairs are decreased by 39% and 29%, respectively, upon the binding of netropsin. In our calculation we used the same interbase H-bond parameters for drug-free and drug-bound DNA. Hence the change in the P^{op} of these pairs is induced either by additional nonbonded interactions introduced by the drug, or by the enhanced cross strand base stacking in the particular crystal netropsin-DNA structure, or a combination of both. To determine which is the dominant factor we include in Table IV a calculation of the P^{op}*s* for the base pairs of a hypothetical drug-free but structurally deformed poly $d(GATATC)$· poly $d(GATATC)$. The conformation of this deformed polymer is taken to be that of the netropsin-bound polymer without the netropsin. A comparison between the P^{op}*s* for the free-deformed DNA and those of the netropsin-bound and drug-free DNA's indicates that the dominant factor for the enhanced thermal stability of the two *AT* pairs is the nonbonded interaction between the binding netropsin and these base pairs.

It is interesting to notice that our calculated P^{op}*s* for the netropsin-bound base pairs are influenced to a certain extent by the specific stacking pattern in the x-ray crystal structure we used to construct our netropsin-DNA model. This is particularly true for the P^{op}*s* for the two *GC* pairs. We find from Table IV that the calculated P^{op}*s* for the two *GC* pairs in the netropsin-bound helix are larger than their counterparts in drug-free DNA. A further look at the P^{op}*s* for the free-deformed DNA shows that the increase is caused by the specific structural feature in the crystal structure. We have carried out a calculation using a nucleic acid structure analysis program [29] to determine structural parameters in our netropsin-DNA structure. The calculated base pair rise and twist angle are given in Table VI. We find that the rise between the *G*1-*C*12 base pair and its two neighbors is substantially larger than the value of 3.38 Å in a standard *B*-conformation DNA. As a result one expects the P^{op} for the *G*1-*C*12 base pair in the particular crystal structure to increase because of weaker stacking interaction with its neighbors. Although the rise between the *C*6-*G*7 base

TABLE VI. Calculated rise and twist between base pairs in netropsin-bound poly $d(GATATC)$·poly $d(GATATC)$. The rise and twist for standard *B*-DNA base pairs are 3.38 Å and 36°, respectively.

Base pair		Rise	Twist
No. 1	No. 2	(Å)	(degree)
*G*1-*C*12	*A*2-*T*11	3.528	31.478
*A*2-*T*11	*T*3-*A*10	3.200	30.716
*T*3-*A*10	*A*4-*T*9	3.383	44.982
*A*4-*T*9	*T*5-*A*8	3.271	25.372
*T*5-*A*8	*C*6-*G*7	3.353	42.653
*C*6-*G*7	*G*1-*C*12	3.676	40.799

pair and one of its neighbors is less than 3.38 Å, the twist is found to be substantially larger than the value of 36° for *B*-form DNA. The larger twist results in a reduced overlapping area between the two base pairs. Therefore one also expects the stacking between the *C*6-*G*7 base pair and its two neighbors to decrease in the crystal structure. This decreased stacking then results in an increase in P^{op}.

VI. CONCLUSION

The dynamics of netropsin binding or dissociation can be analyzed by a statistical approach using microscopic structure and established dynamic force fields. The analysis involves calculations of the disruption of several different elements that bind the drug to the DNA helix. The H bonds between the drug and the bases must be disrupted before the large fluctuation leading to the disruption of other elements. The disruption of the H bonds is induced by fluctuational displacement of tenths of angstroms, which can be easily determined by the cooperative MSPA theory. The van der Waals and Coulomb interactions require much larger displacements for disruption. The disruption of these interaction is a collective process involving many atoms. Such a process can be determined by a self-consistent statistical approach in which the movement of the drug is considered in a composite potential. A unique feature of netropsin dissociation is that it involves conformation change as well as translational separation. Another feature is that Coulomb interactions contribute substantially to the dynamic stability of netropsin binding.

The binding of netropsin is found to affect the thermal stability of the base pairs significantly. The thermal fluctuational opening probability of the base pairs hydrogen bonded to the drug is decreased by orders of magnitude. The probability for the base pairs without drug-base hydrogen bonds is also reduced substantially. In addition the probabilities appear to be influenced by the specific stacking pattern found in the crystal structure. In many biological processes genetic codes are transcribed and replicated from DNA molecules through the separation of base pairs. The understanding of dynamics of drug binding and how drugs enhance the dynamical stability of base pairs can therefore give us insight into the mechanism involved in drug inhibition of these biological processes.

ACKNOWLEDGMENT

This work is supported in part by ONR Grant No. N00014-92-K-1232.

[1] Y. Z. Chen and E. W. Prohofsky, Biophys. J. **66**, 820 (1994).
[2] M. Gueron, D. Broseta, and J.-L. Leroy, Nature (London) **328**, 89 (1987).
[3] Y. Z. Chen and E. W. Prohofsky, Phys. Rev. E **49**, 873 (1994).
[4] M. Techera, Ph.D. thesis, Purdue University, 1991.
[5] E. W. Prohofsky, in *Biomolecular Stereodynamics IV. Proceedings of the Conversation in the Discipline Biomolecular Sterodynamics, 4th, State University of New York at Albany, 1985,* edited by R. H. Samar and M. H. Samar (Adenine, 1986).
[6] C. Zimmer and U. Wahnert, Prog. Biophys. Mol. Biol. **47**, 31 (1987).
[7] R. M. Wartell, J. E. Larson, and R. D. Wells, J. Biol. Chem. **249**, 6719 (1974).
[8] M. L. Kopka, C. Yoon, D. Goodsell, P. Pjura, and R. E. Dickerson, Proc. Natl. Acad. Sci. USA **82**, 1376 (1985).
[9] J. Caldwell and P. Kollman, Biopolymers **25**, 249 (1986).
[10] L. A. Marky and K. J. Breslauer, Proc. Natl. Acad. Sci. USA **84**, 4359 (1987).
[11] M. Coll, J. Aymami, G. A. van der Marel, J. H. van Boom, A. Rich, and A. H.-J. Wang, Biochemistry **28**, 310 (1989).
[12] V. K. Misra, K. A. Sharp, R. A. Friedman, and B. Honig, J. Mol. Biol. **238**, 245 (1994).
[13] M. Gerstein, A. M. Lesk, and C. Chothia, Biochemistry **33**, 6739 (1994).
[14] C. Zimmer, G. Luck, H. Thrum, and C. Pitra, Eur. J. Biochem. **26**, 81 (1972).
[15] K. Zakrzewska, R. Lavery, and B. Pullman, Nucleic Acids Res. **11**, 8825 (1983).
[16] R. Chandrasekaran and S. Arnott, in *Landolt-Bornstein Numerical Data and Functional Relationships in Science and Technology,* edited by W. Saeneger (Springer-Verlag, Berlin, 1989), Vol. VII.
[17] M. Tsuboi, S. Takahashi, and I. Harada, *Physico-Chemical Properties of Nucleic Acids,* edited by J. Duchesne (Academic, New York, 1973), Vol. 2, pp. 91–145.
[18] K. C. Lu, E. W. Prohofsky, and L. L. Van Zandt, Biopolymers **16**, 2491 (1977).
[19] S. J. Weiner, P. A. Kollman, D. A. Case, U. C. Singh, C. Ghio, G. Alagona, S. Profeta, Jr., and P. Weiner, J. Am. Chem. Soc. **106**, 765 (1984).
[20] Y. Z. Chen and E. W. Prohofsky, Biopolymers **33**, 797 (1993).
[21] R. Schroeder and E. R. Lippincott, J. Phys. Chem. **61**, 921 (1957).
[22] W. N. Mei, M. Kohli, E. W. Prohofsky, and L. L. Van Zandt, Biopolymers **20**, 833 (1981).
[23] V. V. Prabhu, L. Young, E. W. Prohofsky, and G. S. Edwards, Phys. Rev. B **39**, 5436 (1989).
[24] S. Califano, *Vibrational States* (Wiley, New York, 1976).
[25] H. M. Berman, S. Neidle, C. Zimmer, and H. Thrum, Biochim. Biophys. Acta **561**, 124 (1979).
[26] K. J. Miller, Biopolymers **18**, 959 (1979).
[27] Y. Z. Chen and E. W. Prohofsky, Phys. Rev. E **48**, 3099 (1993).
[28] Y. Z. Chen and E. W. Prohofsky, Nucleic Acids Res. **20**, 415 (1992).
[29] M. S. Babcock, E. P. D. Pednault, and W. K. Olson, J. Biomol. Struc. Dyn. **11**, 597 (1993).